Title: Fast gamma oscillations weaken with age in healthy elderly in human EEG

Authors: Dinavahi V. P. S. Murty[1], Ranjini Garani Ramesh[1], Simran Purokayastha[1], Mahendra Javali[2], Naren Prahalada Rao[3] and Supratim Ray[1,a].

Affiliations:

[1]Centre for Neuroscience, Indian Institute of Science, Bangalore, India, 560012,

Telephone +91 80 2293 3437, Facsimile +91 80 2360 3323

[2]MS Ramaiah Medical College & Memorial Hospital, Bengaluru, India

[3]National Institute of Mental Health and Neurosciences, Bengaluru, India

[a]**Corresponding Author:** sray@iisc.ac.in

Keywords: Gamma, EEG, Alzheimer's

Conflict of interest: The authors declare no competing financial interests.

Funding Disclosure: This work was supported by Wellcome Trust/DBT India Alliance (500145/Z/09/Z; Intermediate fellowship to SR), Tata Trusts Grant and DBT-IISc Partnership Programme.

Abstract

Gamma rhythms (~20-70 Hz) have been reported to be abnormal in mental disorders such as autism and schizophrenia in humans, and Alzheimer's disease (AD) models in rodents. However, the effect of normal aging on these oscillations is not known, especially for elderly subjects (>49 years) for which AD is most prevalent. In a first large-scale (149 subjects; 61 females) electroencephalogram (EEG) study on gamma oscillations on elderly subjects (aged 50-86 years), we presented full-screen Cartesian gratings that induced two distinct gamma oscillations (slow: 20-34 Hz and fast: 36-66 Hz). Power and centre frequency significantly decreased with age only for fast but not slow gamma or alpha. This result was independent of microsaccades and pupillary reactivity to stimulus. Steady-state visual evoked potentials (SSVEPs) also reduced with age, but in more posterior regions compared to gamma. These results are crucial first steps towards using gamma/SSVEPs as biomarkers of cognitive decline in elderly.

Significance statement

No study in humans has examined visual narrow-band gamma oscillations with healthy aging in elderly subjects. In a first large-scale (~150 subjects) EEG study on stimulus-induced narrow band gamma in cognitively normal elderly (>49 years) humans, we show that both power and centre frequency of fast gamma (36-66 Hz) decrease with age, while changes in other rhythms such as slow gamma (20-34 Hz) or alpha (8-12 Hz) do not. Steady-state visual evoked potential (SSVEPs) in gamma range also decrease with age, but in more posterior regions of the brain. Any EEG-based biomarker is accessible and affordable to patients of a wide socio-economic spectrum. Our results are an important step for developing such screening/diagnostic tests for aging-related diseases, like Alzheimer's disease.

Introduction

Gamma rhythms are narrow-band oscillations often observed in the electrical activity of the brain, with centre frequency occupying ~20-70 Hz frequency range. Previous studies have proposed involvement of these rhythms in certain higher cognitive functions like feature binding (Gray et al., 1989), attention (Gregoriou et al., 2009; Chalk et al., 2010) and working memory (Pesaran et al., 2002). Further, some studies have shown that these rhythms may be abnormal in neuropsychiatric disorders such as schizophrenia (Tada et al., 2014; Hirano et al., 2015), autism (Uhlhaas and Singer, 2007; Wilson et al., 2007; An et al., 2018) and Alzheimer's disease (AD; Palop and Mucke, 2016; Mably and Colgin, 2018).

Gamma rhythms can be induced in the occipital areas by presenting appropriate visual stimuli such as bars and gratings, and their magnitude and centre frequency critically depend on the properties of the stimulus such as contrast, size, orientation, spatial frequency and drift rate (Jia et al., 2013; Ray and Maunsell, 2015; Murty et al., 2018). Recently, we showed that large (full-screen) gratings induce two distinct narrow-band gamma oscillations in local field potentials (LFP) in macaque V1 and posterior electrodes in human EEG, which we termed slow (~20-40 Hz) and fast (~40-70 Hz) gamma (Murty et al., 2018). Fast gamma was not a harmonic of slow, but instead these rhythms were differently tuned to stimulus properties. Importantly, slow gamma was observed only when the grating size was sufficiently large (diameter >8º of visual angle for humans). Two distinct gamma rhythms have also been recently reported in human MEG (Pantazis et al., 2018) and in visual cortex (Veit et al., 2017) and hippocampus (Colgin et al., 2009) in rodents. These rhythms have been suggested to be generated from excitatory-inhibitory interactions of pyramidal cell and interneuron networks (Buzsáki and Wang, 2012), specifically involving parvalbumin (PV) and somatostatin (SOM) interneurons (Cardin et al., 2009; Sohal et al., 2009; Veit et al., 2017).

A recent study has suggested aberrant gamma activity and PV interneuron dysfunction in parietal cortex of AD patients and transgenic models of mice (Verret et al., 2012). However, our knowledge about these rhythms in healthy aging in humans is limited. Studies in human MEG have observed that the centre frequency of gamma oscillations is negatively correlated with age of healthy subjects in the range of 8-45 years (Muthukumaraswamy et al., 2010; Gaetz et al., 2012) although they did not observe any reduction of gamma power with age in this age-group. But our understanding of these rhythms in elderly humans (>49 years), which is clinically more relevant for studying diseases of abnormal aging like AD, is lacking.

Further, visual stimulation of wild type aging and AD models of mice using light flickering at 40 Hz rescued AD pathology in visual cortex (Iaccarino et al., 2016). Such stimulation is known to entrain brain rhythms and generate steady-state visual evoked potentials (SSVEPs) at 40 Hz. However, to our knowledge, no previous study has examined SSVEPs in gamma band in healthy elderly. Furthermore, a recent study has shown flattening of power spectral density (PSD) in 2-24 Hz range in elderly subjects compared to younger subjects (Voytek et. al., 2015). However, how this flattening affects gamma rhythms in elderly has not been examined.

In this study, we described the variation of the two gamma rhythms in healthy elderly subjects. We first used a battery of cognitive tests to identify a large cohort (149 subjects; 61 females) of cognitively healthy elderly subjects aged between 50-86 years. For comparison, we also included 46 younger subjects (aged 20-48 years, 15 females). We induced gamma oscillations using full-screen static Cartesian gratings while monitoring their eye movements and recording EEG, and studied how slow and fast gamma and alpha oscillations, as well as slope of the PSD, varied with age in elderly subjects. In a subset of subjects, we examined SSVEPs in gamma frequency range (32 Hz) as well.

Materials and Methods

Human subjects

We recruited 149 elderly subjects aged 50-86 years from the Tata Longitudinal Study of Aging cohort from urban communities in Bangalore through awareness talks on healthy aging and dementia. Recruitment was done by trained psychologists, who also collected their demographic details. Psychiatrists and neurologists at National Institute of Mental Health and Neurosciences (NIMHANS), Bangalore and M S Ramaiah Hospital, Bangalore assessed the cognitive function of these subjects using a combination of Clinical Dementia Rating scale (CDR), Addenbrook's Cognitive Examination-III (ACE-III), Hindi Mental State Examination (HMSE), and other structured and semi-structured interviews. They ruled out axis-I psychiatric disorders (all psychological disorders except mental retardation, personality disorders and those related to general medical conditions) using Structured Clinical Interview for DSM-IV. We considered only those subjects who were labelled as cognitively healthy for this study.

Further, we also recruited 46 younger subjects from the student and staff community of Indian Institute of Science. We screened them orally for any past history of neurological/psychiatric illness. We had presented data from 10 of these younger subjects in an earlier study (Murty et al., 2018).

All subjects participated in the study voluntarily and against monetary compensation. We obtained informed consent from all subjects for performing the experiment. The Institute Human Ethics Committees of Indian Institute of Science, NIMHANS, Bangalore and M S Ramaiah Hospital, Bangalore approved all procedures.

EEG recordings

Experimental setup, EEG recordings and analysis were similar to what we had described in our previous study (Murty et al., 2018). We recorded raw EEG signals from 64 active

electrodes (actiCAP) using BrainAmp DC EEG acquisition system (Brain Products GmbH). We placed the electrodes according to the international 10-10 system. Raw signals were filtered online between 0.016 Hz (first-order filter) and 1000 Hz (fifth-order Butterworth filter), sampled at 2500 Hz and digitized at 16-bit resolution (0.1 μV/bit). We rejected electrodes whose impedance was more than 25 KΩ. This led to a rejection of 10.2% of electrodes in elderly age-group (1.3% in younger subjects). However, most of these electrodes were frontal/central, and specifically, none were the ten parieto-occipital/occipital electrodes used for analyses (see Data Analysis subsection). Impedance of the final set of electrodes was 5.5±4.5 KΩ (mean±STD) for elderly subjects and 3.6±3.4 KΩ for younger subjects. We referenced EEG signals to FCz during acquisition (unipolar reference scheme).

Experimental setting and behavioral task

All subjects sat in a dark room in front of an LCD screen with their head supported by a chin rest. The screen (BenQ XL2411) had a resolution of 1280 x 720 pixels and a refresh rate of 100 Hz. It was gamma-corrected and was placed at a mean±STD distance of 58.2±1.05 cm (53.9-63.0 cm, 54.9-61.0 cm for the elderly cohort) from the subjects according to their convenience (thus subtending a width of at least 52º and height of at least 30º of visual field for full-screen gratings). We calibrated the stimuli to the viewing distance in all cases.

Subjects performed a visual fixation task. Stimulus presentation was done by a custom software running on MAC OS that also controlled the task flow. Every trial started with the onset of a fixation spot (0.1°) shown at the center of the screen, on which the subjects were instructed to hold and maintain fixation. After an initial blank period of 1000 ms, a series of stimuli (2 to 3) were randomly shown for 800 ms each with an inter-stimulus interval of 700 ms. Stimuli were sinusoidal luminance gratings presented full screen at full contrast. For the main “Gamma” experiment, these were presented at one of three spatial frequencies (SFs): 1,

2, and 4 cycles per degree (cpd) and one of four orientations: 0°, 45°, 90° and 135°. Subjects performed this task in 2-3 blocks (total 410 blocks across 195 subjects) during a single session according to their comfort. For an initial subset of subjects, stimuli with SF of 0.5, 1 and/or 8 were also presented, but we discarded these SFs from further analysis to maintain uniformity. We also tested 32-Hz SSVEPs on a subset of these subjects (144 in elderly and 45 in younger age-groups) according to their willingness for the SSVEP experiment. Gratings (with SF and orientation that showed high change in slow and fast gamma power for each subject) counter-phased at 16 cycles per second (cps) in a similar stimulus presentation paradigm as described above.

Eye position analysis

We recorded eye signals (pupil position and diameter data) using EyeLink 1000 (SR Research Ltd., sampled at 500 Hz) during the entire trial for all but one subject. We calibrated the eye-tracker for pupil position and monitor distance for each subject before the start of the session. All the subjects were able to maintain fixation with a standard deviation of less than 0.5° (elderly, Figure 7a) and 0.3° (young, data not shown). We defined fixation breaks as eye-blinks or shifts in eye-position outside a square window of width 5º centered on the fixation spot. We rejected stimulus repeats with fixation breaks during -0.5s to 0.75s of stimulus onset, either online (and repeated the stimulus thus discarded), or offline (we took a few additional trials to compensate for possible offline rejection), according to the subjects' comfort. This led to rejection of 14.2±12.9% (mean±STD) and 13.9±14.0% trials for elderly subjects (for Gamma and SSVEP experiments respectively), most of who preferred offline rejection. For younger subjects, for many of whom we used online eye-monitoring, the rate of rejection due to fixation breaks was low (4.3±4.8% and 3.8±6.1%).

Artifact rejection

We first discarded bad stimulus repeats separately for each unipolar electrode. We applied a trial-wise thresholding process on both raw waveforms and multi-tapered spectra. For raw waveforms, we first high-pass filtered the signal at 1 Hz to eliminate slow trends if any. We then discarded repeats for which the filtered waveform amplitude within a defined time period of -700 ms to 800 ms of stimulus onset exceeded a threshold of 6 times the standard deviation from the mean amplitude of that repeat (this typically happened during movement or an electrical artifact). We also calculated mean amplitude of the waveforms across repeats in the defined period for every electrode and discarded those trials that exceeded a similar threshold.

For spectral thresholding, we calculated multi-tapered PSD for every repeat (without any offline filters) from -700 ms to 0 ms of stimulus onset using Chronux toolbox (Mitra and Bokil, 2008, http://chronux.org/, RRID:SCR_005547), using 5 tapers. We discarded repeats in which the spectral power in 120-200 Hz range was above a threshold of 3 times the standard deviation from the mean power in that frequency range across all repeats for each electrode separately. We did this to ensure that repeats with flat power spectra (similar to white noise) were discarded. We did this separately for each block for each subject.

In addition, we calculated slopes (see Data Analysis subsection) of PSD (calculated with 1 taper and averaged across repeats, after removal of noisy repeats) for each block in 56 Hz to 84 Hz range (to include the fast gamma range), for the ten unipolar electrodes on which our main analyses were based (see Data Analysis subsection): P3, P1, P2, P4, PO3, POz, PO4, O1, Oz, O2. Previous studies have shown that in clean electrophysiological data, PSD slopes are typically between 0.5 to 4.5 (Podvalny et al., 2015; Shirhatti et al., 2016; Muthukumaraswamy and Liley, 2018; Sheehan et al., 2018). We therefore discarded blocks (67/410, i.e. 16.3% from Gamma experiment, shown in Figure 2a) that did not have mean slopes between 0.5-4.5 and standard deviation of <3 across the ten electrodes described above. We then pooled data across

all good blocks for every subject separately for final analysis. Those subjects who did not have any analyzable blocks in the Gamma study (21/149 and 2/46 for elderly and younger subjects respectively) were discarded from further analysis, leaving 128 elderly (aged 50-86 years, mean±STD: 66.3±8.0 years, females: 56) and 44 young subjects (aged 20-48 years, mean±STD: 30.0±7.0 years, females: 15) for analysis. Out of these, 98 elderly (mean±STD: 65.9±7.8 years, females: 46) and 38 young (mean±STD: 30.1±7.3 years, females: 12) subjects had analyzable blocks (135/166, i.e. 81.3%) for SSVEP experiment.

Overall, within analyzed blocks, there were 33.7±8.2 (mean±STD) and 39.5±6.6 repeats (for Gamma and SSVEP experiments) for every stimulus across all elderly subjects (31.3±6.8 and 34.1±7.9 for young subjects) during recording across all analyzable unipolar electrodes (i.e., those electrodes with impedance <25 KΩ). From these, we rejected 18.0±14.6% and 17.1±16.1% of repeats (mean±STD, for Gamma and SSVEP experiments respectively, including those discarded for fixation breaks as explained above) for elderly subjects and 7.4±7.7% and 6.5±7.9% for younger subjects. Therefore, in spite of our stringent criteria for bad trial rejection, more than 80% of the data could be used for analysis.

EEG data analysis

For all analyses (unless otherwise mentioned), we used bipolar reference scheme. We re-referenced data at each electrode offline to its neighboring electrodes. We thus obtained 112 bipolar pairs out of 64 unipolar electrodes (Murty et al., 2018, depicted in Figure 3e). For each of these bipolar electrodes, we considered the union of bad stimulus repeats for the two constituting unipolar electrodes as bad for that bipolar electrode and rejected from analysis. Further, we discarded a bipolar electrode if either of its constituting unipolar electrodes had impedance >25 KΩ. Overall, there were 27.1±8.3 and 31.9±8.4 trials (mean±STD, for Gamma and SSVEP experiments respectively) per stimulus condition across all useful bipolar

electrodes for elderly subjects and 27.5±6.5 and 31.0±7.1 trials for younger subjects. Further, there was no significant correlation between the number of trials and age. We considered the following bipolar combinations for analysis, except for scalp maps: PO3-P1, PO3-P3, POz-PO3 (left anterolateral group); PO4-P2, PO4-P4, POz-PO4 (right anterolateral group) and Oz-POz, Oz-O1, Oz-O2 (posteromedial group), depicted in Figure 3d.

We analyzed all data using custom codes written in MATLAB (The MathWorks, Inc, RRID:SCR_001622). We computed PSD and the time-frequency power spectrograms using multi-taper method with a single taper using Chronux toolbox. We chose baseline period between -500 ms to 0 ms of stimulus onset, while stimulus period between 250 ms to 750 ms to avoid stimulus-onset related transients, yielding a frequency resolution of 2 Hz for the PSDs. We calculated time frequency power spectra using a moving window of size 250 ms and step size of 25 ms, giving a frequency resolution of 4 Hz.

We calculated change in power in alpha rhythm and the two gamma rhythms as follows:

$$\Delta\mathrm{Power}_{\mathrm{i,j}} = 10\left(\log_{10}\mathrm{ST}_{\mathrm{i,j}} - \mathrm{BL}_{\mathrm{ave}}\right), \text{ where } \mathrm{BL}_{\mathrm{ave}} = \frac{1}{i.j}\sum_i\sum_j(\log_{10}\mathrm{BL}_{\mathrm{i,j}})$$

Here, $\mathrm{ST}_{\mathrm{i,j}}$ and $\mathrm{BL}_{\mathrm{i,j}}$ are stimulus and baseline PSD powers summed across the frequency range of interest (excluding 50 Hz for line noise) for each of the rhythms for spatial frequencies $i \in$ [1, 2, 4 cpd] and orientations $j \in$ [0º, 45º, 90º, 135º]. We then averaged change in power across the 3 SFs and 4 orientations to yield the final change in power in each band. Note that due to this averaging, on average more than 200 stimulus repeats were available for analysis, yielding very reliable estimates. For calculating center frequency of gamma rhythms, we used the average change in PSD across spatial frequencies and orientation. We then defined the center frequency for a gamma rhythm as the frequency at which the change in power was maximum within that gamma range. For SSVEP experiment, there was only one condition: grating counter-phasing at 16 cps. Hence, we took the power at 32 Hz frequency for analysis.

We generated scalp maps using the topoplot.m function of EEGLAB toolbox (Delorme and Makeig, 2004, RRID:SCR_007292), modified to show each electrode as a colored disc, with color representing the change in power of slow gamma/fast gamma/SSVEP from baseline in decibels (dB).

For Figure 2, we calculated slopes for baseline PSDs from SF-orientation experiments as mentioned in a previous study (Shirhatti et al., 2016). We fitted the average PSD across all 9 bipolar/10 unipolar electrodes with a power-law function as follows:

$$P(f) = A.f^{-\beta} + C$$

where P is the PSD across frequencies $f \in [16\ 44]$ Hz. A (scaling factor), β (slope) and C (noise floor) are free parameters obtained using least square minimization using the program *fminsearch* in MATLAB.

Statistical analysis

We performed Pearson correlation (and/or linear regression) analysis with an assumption of normal distribution of data as the sample size was large (for example, 172 for Supplementary Figure 1b; 128 for Figures 4c, 4d, 5c and 5d; 87 for 6b top row; 70 for 6b bottom row; 127 for 7a and 7d; 105 for 7c and 98 for 8c). We used one-way (or two-way, as necessary) ANOVA to compare means of bar plots in Figures 2d, 4c, 4d, 5c, 5d and 8c, although non-parametric tests on medians instead of means using Kruskal-Wallis test (not reported) yielded qualitatively similar results. We used Bonferroni correction for multiple tests/comparisons wherever necessary.

Microsaccades and pupil data analysis

We detected microsaccades using a threshold-based method described earlier (Murty et al., 2018), initially proposed by (Engbert, 2006). In brief, we categorized eye movements with

velocities that crossed a specified threshold for at least a specified duration of time as microsaccades. We set the velocity threshold between 3-6 times the standard deviation of eye-velocities and minimum microsaccade duration between 10-15 ms for every subject so as to maximize the correlation between peak velocity and amplitude of all microsaccades for that subject (also called a “main sequence”, see Engbert, 2006 for details), while maintaining the minimum microsaccade velocity at 10º/s and the microsaccade rate between 0.5/s and 3.0/s.

The above algorithm was applied for the analysis period of -0.5 s to 0.75 s of stimulus onset. After removing the microsaccade-containing trials, there were 105 subjects with at least 2 analyzable trials (mean±SEM: 14.0±6.8) across all conditions for anterolateral electrodes reported in Figure 7c.

EyeLink 1000 system recorded pupil data in arbitrary units for every subject since pupil data cannot be calibrated for this tracker. Hence, instead of directly comparing time-series of pupil data, we used coefficient of variation (CV, ratio of standard deviation to mean) for every repeat as a measure of pupillary reactivity to stimulus of that repeat. This simple measure scales standard deviation of a distribution with respect to its mean. This allows comparison of variation in different distributions without getting affected by the mean of the distributions. We calculated CV for each analyzable trial separately and calculated mean CV across trials for every subject for comparison.

Results

We recorded EEG from 149 elderly subjects aged 50-86 years and 46 subjects aged 20-49 years while presenting full-screen sinusoidal grating stimuli on a computer monitor. The stimuli differed in spatial frequency and orientation. Each stimulus was presented for 800 ms following a baseline period of 700 ms. The subjects were required to maintain fixation throughout the trial (containing 2-3 stimuli), while their eye-data was recorded for offline analysis. For analysis, we pooled the data across the four orientations (0º, 45º, 90º, 135º) for all subjects, as orientation selectivity was reported to be very low for humans for both slow and fast gamma bands (Murty et al., 2018). Similarly, we pooled across three spatial frequencies (1-4 cpd) which were reported to elicit salient gamma oscillations in humans (Murty et al., 2018).

Figure 1 shows the results of an example subject, a 53 years old female. Trial-averaged evoked potentials were plotted (Figure 1a) for electrodes P3, P1, P2, P4, PO3, POz, PO4, O1, Oz, O2 for unipolar reference (Figure 1a, left column) and PO3-P1, PO3-P3, POz-PO3, PO4-P2, PO4-P4, POz-PO4, Oz-POz, Oz-O1 and Oz-O2 (shown as dots in scalp maps in Figure 1c) for bipolar reference (Figure 1a, right column). These traces revealed a transient in the first 250 ms of stimulus onset and after the stimulus offset (i.e. after 800 ms). For the same set of electrodes, trial-wise power spectrograms were averaged to generate raw spectrogram and change in power spectrogram (w.r.t. a baseline period of -500 ms to 0 ms of stimulus onset), plotted in Figure 1a. Although not noticeable in the evoked potential traces and raw spectrograms, these stimuli elicited prominent gamma band responses as seen in the change in power spectrograms. These responses were in slow gamma (~20-34 Hz) and fast gamma (~36-66 Hz) range. Consistent with previous results (Murty et al., 2018), these responses were seen during the stimulus period (after the onset-transient) and were best noticed for bipolar reference (compared to unipolar reference). Also, slow gamma power showed a gradual build-up whereas

fast gamma power showed a decreasing trend with stimulus duration (Figure 1a, bottom row). Interestingly, alpha (8-12 Hz) power suppression was very weak in this subject. We also plotted power spectral densities (PSD) in the baseline period (dotted black trace in Figure 1b) and stimulus period (250 ms to 750 ms; solid black trace in Figure 1b) and change in power spectrum (blue trace in Figure 1b). Prominent 'bumps' in the slow and fast gamma range were noticeable in PSD in the stimulus period as well as change in spectrum. Also, no 'bump' was noticeable in the baseline PSD in the alpha range for this subject. These changes were most prominent in the parieto-occipital and occipital electrodes, as seen in the scalp maps for the bipolar reference case in Figure 1c.

For accurate estimation of gamma (especially fast gamma), it is essential that the power in the gamma range of the EEG signal is above the noise floor. For noisy EEG, we observed that the PSDs tended to become flat, potentially because of white noise. Therefore, we chose only those blocks for analysis (343 out of 410 blocks recorded from 195 subjects) that had mean baseline PSD slopes between 56-84 Hz in the range of 0.5-4.5 and standard deviation <3 across 10 electrodes listed above for unipolar reference (Figure 2a). Subjects who did not have any usable blocks were removed from analysis, leaving 128 elderly (56 females) and 44 young (15 females) subjects. For these subjects, we then pooled data across all useful blocks to compute the power.

Note that the younger subjects were from a different cohort compared to the elderly subjects and did not go through the cognitive tests or clinical evaluation that elderly subjects went through (some of these tests were not even applicable to them). Therefore, while we show and analyse all results for younger subjects (aged 20-49 years) for completeness, our primary emphasis was to characterize gamma and other spectral signatures as a function of age within the elderly population (>49 years), for which we divided these subjects into two groups: 50-64 years (55 subjects; 32 female) and >64 years (73 subjects, 24 female).

Baseline power of slow and fast gamma did not vary with age

A recent study (Voytek et al., 2015) has suggested rotation of PSDs with age such that power at frequencies above ~15 Hz is higher in elderly subjects compared to younger subjects, leading to flatter PSDs in elderly subjects. This could potentially bias the estimation of change in power in slow and fast gamma range in subjects of different age groups as higher baseline power in these rhythms in older subjects may lead to lower estimates of change in power. Hence, we first checked whether there was any difference in baseline PSDs across age. We calculated mean baseline PSDs of 10 unipolar electrodes and 9 bipolar electrodes separately. We compared PSDs between 2-200 Hz in the two elderly groups as well as the younger group (Figure 2b), and males versus females (averaged across all ages; Figure 2c).

Because our primary emphasis was comparison within the elderly group, we first compared the PSDs between the two elderly subgroups, and found them to be very similar (dark and light gray traces in Figure 2b). We performed a two-way ANOVA on alpha, slow gamma and fast gamma with age-group (50-64 or >64 years) and gender as factors and found that age group was not significant for any band ($p>0.05$ in all cases). We also computed Pearson correlation between baseline alpha/slow/fast gamma power and age and did not find significant correlation in any condition.

As observed in Figure 2b, the main difference was a significantly higher ‘bump’ in the alpha range in younger subjects versus elderly, while the PSDs were largely overlapping in other frequency bands. Also, females had higher power than males up to ~50 Hz but not for higher frequencies (Figure 2c). We quantified this by using a two-way ANOVA with age-group (20-49 or >49 years) and gender as factors. Baseline alpha power was lower in the elderly subjects compared to the younger subjects ($F(1,169)=9.1$, $p=0.003$ and $F(1,169)=7.2$, $p=0.008$ for unipolar and bipolar reference), but there was no significant difference in baseline power

in slow/fast gamma ranges ($p>0.07$ in all cases; Figure 2b). Between males and females, the difference in baseline power was significant in alpha and slow gamma ranges, but not for fast gamma (alpha/slow/fast gamma: $F(1,169)=6.8/25.5/5.5$, $p=0.01/1.1*10^{-6}/0.02$ and $F(1,169)=7.4/27.8/0.9$, $p=0.007/4.1*10^{-7}/0.3$ for unipolar and bipolar reference, significance level set to 0.05/4 = 0.0125 after Bonferroni correction).

We did not find any rotation of the PSD with age as reported previously (Voytek et al., 2015). To quantify this, we computed the slopes between 16-44 Hz (see Methods for details; this range was chosen to avoid the bump in the alpha band at the lower end and the 50 Hz noise at the higher end, and also because the PSDs were overlapping beyond 50 Hz). Two-way ANOVA with age (young and elderly) and gender (male and female) as factors showed no significant difference in the slopes between young and elderly subjects for either unipolar or bipolar reference scheme case ($p>0.3$). However, females had steeper slopes compared to males (two-way ANOVA as above, $F(1,169)=6.1$, $p=0.014$ and $F(1,169)=24.6$, $p=1.7*10^{-6}$ for unipolar and bipolar cases respectively). Since females had higher baseline alpha power compared to males (Figures 2c), we tested whether any differences in baseline PSD slopes could be because of differences in baseline alpha power. We divided baseline PSDs of all subjects (young and elderly pooled together) into terciles based on alpha power (Figure 2d). Subjects who had higher baseline alpha power also had steeper PSD slopes. Regression of PSD slopes in 16-44 Hz frequency range with baseline alpha power was significant for both reference schemes (Supplementary Figure 1b). Further, when we performed partial correlation of slopes with age and baseline alpha power, slopes were significantly correlated with alpha power (rho=0.55, $p=1.0*10^{-14}$ and rho=0.58, $p=4.1*10^{-17}$ for unipolar and bipolar cases respectively) but not with age (rho=0.12 and -0.02 for unipolar and bipolar, $p>0.1$ for both). Thus, PSD slope was not influenced by age, but by baseline alpha power. We discuss these results in the context of the findings of Voytek and colleagues in the Discussion.

Gamma was observed in more than 80% of subjects

As reported in our earlier study (Murty et al., 2018) and as in Figure 1, gamma was best observed, as a response to full-screen 100% contrast cartesian visual gratings, in bipolar referencing scheme compared to unipolar. Hence, we limited further analysis to bipolar referencing. We divided the 9 bipolar electrodes mentioned above into 3 groups (Figure 3d): PO3-P1, PO3-P3, POz-PO3 (left anterolateral group); PO4-P2, PO4-P4, POz-PO4 (right anterolateral group) and Oz-POz, Oz-O1, Oz-O2 (posteromedial group). For each subject, we chose the electrode group that had maximum change in power in slow and fast gamma ranges added together. We labelled a subject as having either of the gamma rhythms if the change in power in these rhythms during stimulus period (calculated from data pooled across electrodes chosen for the subject) exceeded an arbitrarily chosen threshold of 0.5 dB from baseline. Figure 3a shows scatter plot of slow versus fast gamma change in power for all subjects. Based on our threshold, ~84% of subjects had at least one gamma (slow: ~76% and fast: ~76%), while ~60% of subjects had both the gammas, which could be observed as distinct “bumps” in the change in PSD from baseline (Figure 3b). Figure 3c shows the percentage of subjects in each age-group who had no/slow/fast/both gammas based on our threshold. The percentage of subjects who had only fast gamma or both gammas was highest in 20-49 years age-group and lowest in >64 years age-group.

Figure 3e shows change in power in slow (top row) and fast (bottom row) gamma rhythms across all electrodes (plotted as disks) for the young (left column) and the two elderly age-groups (middle and right columns). Both gamma rhythms were best observed in the same 9 bipolar electrodes mentioned above and depicted in Figures 3d and 3e. Further, while there was no discernible difference in slow gamma power in these electrodes, fast gamma appeared to decrease with age across the two elderly age-groups.

Change in fast gamma power was negatively correlated with age

To quantify this difference, we tested how gamma oscillations correlated with age in these electrode groups. We tested for anterolateral and posteromedial groups separately (Figures 4 and 5 respectively). For Figure 4, out of the left and right anterolateral groups, we chose that group which had maximum slow and fast gamma power change summed together. Figures 4a and 4b show mean change in spectrograms and PSDs respectively for the three age-groups separately for males and females. Left columns of Figures 4c and 4d show bar plots for change in power in slow and fast gamma power across the three age groups for males and females.

Younger subjects had significantly more fast (but not slow) gamma than elderly subjects (two-way ANOVA with age-group (20-49 and >49 years) and gender as factors, $F(1,169)=2.3/34.9$, $p=0.1/1.8*10^{-8}$ for slow/fast gamma). Moreover, females had more fast (but not slow) gamma than males (same two-way ANOVA, $F(1,169)=3.2/33.2$, $p=0.07/3.9*10^{-8}$ for slow/fast gamma). Interestingly, while visual inspection of change in spectrograms and spectra revealed that fast gamma power was less in males of >64 years age-group compared to 50-64 years age-group, the difference was not noticeable in females. Slow gamma remained comparable in both the elderly age-groups for both genders. We quantified these observations by regressing change in slow and fast gamma power across age separately for elderly males and females (data not shown). Regression slope was negative ($\beta=-0.018$) and significant ($p=0.0049$) for fast gamma in elderly males, but not in other cases. However, there are two points to note in our data. First, number of females was less than number of males in younger (male:female = 29:15) and >64 years (49:24) age-groups. Second, most of the elderly females were less than 70 years of age (median age for males and females was 69 and 62.5 years respectively for subjects >49 years of age), leading to lower age-range compared to males. The

unequal sample size and narrow age range of females could have affected the regression slope and significance of fast gamma power change across age.

To avoid such statistical misinterpretation and because the main objective of our study was to study the variation of gamma power across age (and not gender), we pooled data across both genders and two elderly age groups and then regressed slow and fast gamma power with age (Figures 4c and 4d: right columns). Fast gamma power change reduced significantly with age (linear regression, β=-0.02, R^2=0.06, p=0.0055), whereas slow gamma power change did not (β=-0.01, R^2=0.01, p=0.23). Similar, albeit weaker results were observed in the posteromedial group of electrodes for fast gamma (Figure 5d; linear regression, β=-0.016, R^2=0.03, p=0.038) as well as slow gamma (Figure 5c; β=-0.012, R^2=0.014, p=0.18).

<u>Centre frequency of fast gamma was negatively correlated with age</u>

Gamma peak centre frequency has been shown to decrease with age in an age group between 8-45 years (Muthukumaraswamy et al., 2010; Gaetz et al., 2012). This was observed in our data as well: visual inspection of Figure 4b and 5b shows a decrease in centre frequency in fast gamma between the three age-groups. To examine the change in centre frequency of slow and fast gamma rhythms in elderly in more detail, we plotted the change in power spectra (frequencies mentioned on abscissa) vs age (on ordinate, arranged in increasing order from top to bottom) of all 128 elderly subjects, separately for anterolateral (left column) and posteromedial (right column) group of electrodes. We defined centre frequency for each gamma as the frequency that had maximum change in power in the frequency range of that gamma, provided the total change in power in that gamma band was greater than our threshold of 0.5 dB (represented by circles and triangles for slow and fast gamma in Figure 6a; 87 and 70 subjects had slow and fast gamma power change above this threshold). Figure 6b shows the

same result as scatter plots of centre frequencies of slow gamma of these 87 subjects (top row) and fast gamma of 70 subjects (bottom row) plotted against the age of the subjects. Solid lines in Figures 6a and 6b indicate regression fits of centre frequencies against age (showing decreasing trends), which were significant for fast gamma (linear regression, β=-0.24, R^2=0.13, p=0.003 for posterolateral group and β=-0.19, R^2=0.09, p=0.01 for anterolateral group, Figure 6b bottom row), but not for slow gamma (β=-0.038, R^2=0.01, p=0.29 for posterolateral group and β=-0.034, R^2=0.008, p=0.39 anterolateral group, Figure 6b top row).

<u>Microsaccades and pupillary reactivity did not contribute to negative correlation of change in fast gamma power and age</u>

Next, we studied the potential contribution of eye-movement including microsaccades and pupillary diameter on our results. Figure 7a shows mean eye-position for each of the elderly age-groups in horizontal (top row) and vertical (middle row) directions (thickness represent SEM). Eye-position did not vary in the two age-groups in either direction. Further, we extracted microsaccades for every analysed trial for every subject in the two age-groups (see Materials and Methods), yielding a total of 21051 and 25748 microsaccades for the two age-groups. Figure 7b shows a scatter plot of peak velocity versus maximum displacement for each microsaccade (a plot called “main sequence”, see Engbert, 2006). These plots were highly overlapping for these two groups. Both the elderly groups had similar microsaccade rates (0.83±0.06/s and 0.87±0.06/s). Histograms of microsaccade rate during -0.5 – 0.75 s of stimulus onset for both the elderly age-groups were also highly overlapping (Figure 7a, bottom plot). As an additional control, we computed power after first removing trials containing microsaccades (see Materials and Methods for details), and could replicate the results in Figure 4: change in fast gamma power decreased with age significantly whereas slow gamma did not

(β=-0.01, R^2=0.01, p=0.33 for slow gamma and β=-0.02, R^2=0.04, p=0.03 for fast gamma, Figure 7c).

We next tested if pupillary reactivity to stimulus presentation affected change in gamma power with age. We calculated mean coefficient of variation (CV) of pupil diameter across every analysable trial for all 127 subjects (eye data was unavailable in one subject). We observed that mean CV decreased significantly with age in the elderly subjects, possibly because of senile miosis (Pearson correlation, r=-0.21, p=0.02, Figure 7d top row). However, neither slow nor fast gamma power varied with mean CV of pupil diameter (slow/fast: r=0.02/0.06, p=0.83/0.52 and r=0.03/0.12, p=0.71/0.18 for anterolateral and posteromedial electrodes respectively).

<u>32 Hz SSVEP power was negatively correlated with age</u>

Finally, we checked whether SSVEPs in the gamma range were affected by healthy aging. Specifically, we used 32-Hz SSVEPs elicited by gratings counter-phasing at 16 cps. Figure 8a and 8b show change in power spectrograms and spectra respectively for males and females separately for the two elderly and the younger age-groups for the posteromedial group of electrodes, with same conventions as in Figures 4 and 5. We see clear peaks in change in power at 32 Hz in both spectrograms and PSDs (Figure 8b). Insets in Figure 8b show a zoomed-in image of the respective change in PSDs to show the difference in these peaks for the three age-groups. Amongst the elderly age-groups, the mean SSVEP change in power was less in the >64 years age-group compared to 50-64 years age-group in both males and females, although the trend seemed to be more significant for males. Same is reflected in the bar plots in Figure 8c (top row). We pooled data across both genders for the two elderly age-groups and regressed the SSVEP power change with age (scatter plot in Figure 8c bottom row). Change in SSVEP

power at 32 Hz decreased significantly with age for both posteromedial and anterolateral group of electrodes, although the effect was stronger for the former (β=-0.14, R^2=0.08, p=0.004 for posterolateral group and β=-0.12, R^2=0.05, p=0.03 for anterolateral group, data not shown). We noticed the same in the mean scalp maps for all analysable electrodes across all subjects in the three age-groups depicted in Figure 8d.

Discussion

We tested for age-dependent variation of stimulus-induced change in power and centre frequency of narrow-band gamma oscillations in both slow and fast gamma frequency ranges in healthy elderly subjects aged 50-86 years. While power in fast gamma oscillations decreased with age, we did not observe such a variation for slow gamma. Moreover, this decrease was most prominent in anterolateral group of electrodes, compared to the posteromedial ones in the parieto-occipital and occipital regions. Centre frequency of fast gamma, but not slow gamma, decreased with age in these subjects. As there was no significant change in baseline slow/fast gamma power, eye-position and microsaccade rate across age, we ruled out the possibility that the age-related variations in gamma could be because of such factors. Further, we also studied variation of 32 Hz SSVEP power with age and noticed negative correlation, especially in the posteromedial group of electrodes. All these results were also analysed for a cohort of younger subjects (aged 20-48), and the results were consistent with previous reports on gamma oscillations and some of the trends observed in the elderly population.

Baseline alpha power and PSD slopes

Previous studies have suggested reduction in baseline alpha power in elderly subjects compared to younger subjects in the eyes-closed state (Babiloni et al., 2006). Also, task-related modulation of alpha power was seen to be reduced in older adults compared to younger subjects (Vaden et al., 2012). In our study, we observed that baseline alpha power in the elderly was less than that for young subjects; however, it did not fall further amongst the elderly age-group (Figure 2b). Similarly, alpha suppression during the stimulus presentation was less in elderly age-groups compared to young subjects (as observed in change in power spectrum and

spectrogram plots in Figures 4 and 5). This could be possibly because of low baseline alpha power to begin with.

Some authors have suggested that power-law distribution ($1/f^{\beta}$, where β is the PSD slope) of brain electrical activity represents broadband scale-free activity of brain that is dependent on behavioral states (He et al., 2010; He, 2014; Podvalny et al., 2015) and cognitive abilities (Voytek et al., 2015; Sheehan et al., 2018). Specifically, Voytek et al. had suggested that flattening of PSD slopes might be a hallmark of senile physiological cognitive decline. In our study however, we did not notice any correlation between baseline PSD slopes and age, especially for elderly subjects. There are several reasons that could have led to this discrepancy. First, the sample size of Voytek and colleagues was small (11 young and 13 elderly) with a larger proportion of females in the younger group (male:female = 4:7 and 8:5 in young and elderly groups). Because females had steeper slopes than males (Figure 2d), underrepresentation of females in the elderly group could have led to flatter PSDs in their data. Second, we found that PSD slopes were correlated with baseline alpha power, which was higher in younger versus elderly. A similar correlation of slopes with alpha power was also reported by Muthukumaraswamy and Liley (2018) in human MEG and EEG as well as monkey ECoG. Importantly, these parameters (broadband slopes and alpha power) were indistinguishable in the two elderly age-groups (50-64 and >64 years) over which most of our analyses were carried out.

Possible confounds from ocular factors

Broadband induced gamma responses have been proposed to be correlated with occurrence of microsaccades (Yuval-Greenberg et al., 2008). However, in our previous study, we did not note any effect of microsaccades on orientation tuning of narrow-band slow and fast

gamma oscillations in macaques (Murty et al., 2018). Consistently, we did not find any effect of microsaccades on age-dependent decrease of fast gamma power in this study.

It is possible that retinal illuminance is reduced due to senile pupillary miosis, which is indirectly reflected in the reduced pupillary reactivity to stimulus presentation across age (Figure 7c). Other abnormalities of peripheral visual system age-related increase in density of crystalline lens, age-related macular degeneration, etc. could have had affected our results (Owsley, 2011). The subjects did not undergo a thorough ophthalmic examination due to the limitations of the study. However, we argue that the results presented here are likely due to neurophysiological effects of aging on three grounds. First, in addition to a reduction in fast gamma power, there is a reduction in gamma centre frequency with age, which is harder to explain based on the abnormalities listed above. Second, any pathology in the eye should have had affected slow gamma, fast gamma and SSVEPs in similar ways, which is not the case here: slow gamma did not vary with age, and fast gamma and SSVEP showed variation with age more strongly in different groups of electrodes (anterolateral and posteromedial, respectively). Third, slow/fast gamma power was not dependent on pupillary reactivity to stimulus (Figure 7d).

<u>Slowing of both gamma rhythms with age</u>

We observed that slow and fast gamma ‘bumps’ in change in PSD plots (in both Figures 4b and 5b) moved leftwards, especially between younger subjects and elderly. We could have chosen the gamma band frequency limits differently for each condition/subject, but this could have made the final results dependent on these choices. Hence, we fixed the slow and fast gamma ranges for all subjects at 20-34 Hz and 36-66 Hz. Clearly, the mean change in power at 20 Hz for >64 years age group was slightly higher than that for other age-groups, especially

for females (light grey trace in Figures 4b and 5b). This has important implications for calculation of gamma power. Because raw power falls off with increasing frequency, the overall band power is influenced by the power at lower frequency limit of the band. This could be one reason that the mean change in slow gamma power seemed higher for females of >64 years age-group than other age-groups in bar plots in Figures 4c and 5c, even though the younger subjects have a taller peak (at ~28 Hz) than the two elderly groups (Black trace in Figures 4b and 5b). However, we did not observe the negative trend of slow gamma with age to be significant (Figure 6b). This could be because of two reasons: firstly, the frequency resolution of our analysis was limited to 2 Hz. Moreover, slow gamma frequency range itself is small, spanning 14 Hz. This may have limited the significance of the trend given the large variance.

Possible mechanisms of age-related reductions in fast gamma frequency and change in power

Previous studies in MEG had reported significant positive correlations between (fast) gamma frequency and cortical thickness as well as volume of cuneus (Gaetz et al., 2012) and thickness of pericalcarine area (Muthukumaraswamy et al., 2010), measured through structural MRI. Further, age-related decreases in cortical volume, thickness and/or surface area were observed in various regions of the brain like precuneus, cuneus, lingual, pericalcarine and lateral occipital areas of the occipital cortex (Salat et al., 2004; Lemaitre et al., 2012). In line with these observations, these MEG studies have also noted decrease of centre frequency of gamma with age, esp. in young and middle-aged adults. Similarly, (fast) gamma peak frequency has been positively correlated with brain GABA levels (Edden et al., 2009; Muthukumaraswamy et al., 2009). Although we have not tested directly for these variables in our study, we speculate that these morphological and neurochemical factors are the reasons for

our observations regarding fast gamma frequency. However, the factors behind relative invariance of slow gamma with age remains an open question.

To conclude, our study throws light on various features of baseline spectra (like baseline alpha power and its relation to PSD slopes) and spectral responses to Cartesian gratings (slow and fast gamma) in a large cohort of healthy elderly. Our study could thus act as normative for future gamma and SSVEP studies in the elderly age-group. Further, based on observations in previous rodent studies (for example, Verret et al., 2012; Iaccarino et al., 2016) as described before, some authors have suggested a causative role of (fast) gamma disruption in neurodegenerative disorders of aging such as AD (Palop and Mucke, 2016). Alternatively, our results suggest that fast gamma and SSVEPs suffer reduction in power with age even in the absence of cognitive decline. These studies taken together, decrease in fast gamma/SSVEP power may represent a continuum of healthy aging – preclinical cognitive decline – dementia spectrum and may act as a harbinger to senile or pathological cognitive decline, a hypothesis that needs to be tested in future studies.

References

An K, Ikeda T, Yoshimura Y, Hasegawa C, Saito DN, Kumazaki H, Hirosawa T, Minabe Y, Kikuchi M (2018) Altered Gamma Oscillations during Motor Control in Children with Autism Spectrum Disorder. J Neurosci 38:7878–7886.

Babiloni C, Binetti G, Cassarino A, Forno GD, Percio CD, Ferreri F, Ferri R, Frisoni G, Galderisi S, Hirata K, Lanuzza B, Miniussi C, Mucci A, Nobili F, Rodriguez G, Romani GL, Rossini PM (2006) Sources of cortical rhythms in adults during physiological aging: A multicentric EEG study. Hum Brain Mapp 27:162–172.

Buzsáki G, Wang X-J (2012) Mechanisms of Gamma Oscillations. Annu Rev Neurosci 35:203–225.

Cardin JA, Carlén M, Meletis K, Knoblich U, Zhang F, Deisseroth K, Tsai L-H, Moore CI (2009) Driving fast-spiking cells induces gamma rhythm and controls sensory responses. Nature 459:663–667.

Chalk M, Herrero JL, Gieselmann MA, Delicato LS, Gotthardt S, Thiele A (2010) Attention Reduces Stimulus-Driven Gamma Frequency Oscillations and Spike Field Coherence in V1. Neuron 66:114–125.

Colgin LL, Denninger T, Fyhn M, Hafting T, Bonnevie T, Jensen O, Moser M-B, Moser EI (2009) Frequency of gamma oscillations routes flow of information in the hippocampus. Nature 462:353–357.

Delorme A, Makeig S (2004) EEGLAB: an open source toolbox for analysis of single-trial EEG dynamics including independent component analysis. J Neurosci Methods 134:9–21.

Edden RAE, Muthukumaraswamy SD, Freeman TCA, Singh KD (2009) Orientation Discrimination Performance Is Predicted by GABA Concentration and Gamma Oscillation Frequency in Human Primary Visual Cortex. J Neurosci 29:15721–15726.

Engbert R (2006) Microsaccades: a microcosm for research on oculomotor control, attention, and visual perception. In: Progress in Brain Research (Martinez-Conde S, Macknik SL, Martinez LM, Alonso J-M, Tse PU, eds), pp 177–192 Visual Perception. Elsevier. Available at: http://www.sciencedirect.com/science/article/pii/S0079612306540099 [Accessed November 12, 2017].

Gaetz W, Roberts TPL, Singh KD, Muthukumaraswamy SD (2012) Functional and structural correlates of the aging brain: Relating visual cortex (V1) gamma band responses to age-related structural change. Hum Brain Mapp 33:2035–2046.

Gray CM, König P, Engel AK, Singer W (1989) Oscillatory responses in cat visual cortex exhibit inter-columnar synchronization which reflects global stimulus properties. Nature 338:334–337.

Gregoriou GG, Gotts SJ, Zhou H, Desimone R (2009) High-Frequency, Long-Range Coupling Between Prefrontal and Visual Cortex During Attention. Science 324:1207–1210.

He BJ (2014) Scale-free brain activity: past, present, and future. Trends Cogn Sci 18:480–487.

He BJ, Zempel JM, Snyder AZ, Raichle ME (2010) The Temporal Structures and Functional Significance of Scale-free Brain Activity. Neuron 66:353–369.

661 Hirano Y, Oribe N, Kanba S, Onitsuka T, Nestor PG, Spencer KM (2015) Spontaneous Gamma Activity
662 in Schizophrenia. JAMA Psychiatry 72:813–821.

663 Iaccarino HF, Singer AC, Martorell AJ, Rudenko A, Gao F, Gillingham TZ, Mathys H, Seo J, Kritskiy O,
664 Abdurrob F, Adaikkan C, Canter RG, Rueda R, Brown EN, Boyden ES, Tsai L-H (2016) Gamma
665 frequency entrainment attenuates amyloid load and modifies microglia. Nature 540:230.

666 Jia X, Tanabe S, Kohn A (2013) Gamma and the Coordination of Spiking Activity in Early Visual Cortex.
667 Neuron 77:762–774.

668 Lemaitre H, Goldman AL, Sambataro F, Verchinski BA, Meyer-Lindenberg A, Weinberger DR, Mattay
669 VS (2012) Normal age-related brain morphometric changes: nonuniformity across cortical
670 thickness, surface area and gray matter volume? Neurobiol Aging 33:617.e1-617.e9.

671 Mably AJ, Colgin LL (2018) Gamma oscillations in cognitive disorders. Curr Opin Neurobiol 52:182–
672 187.

673 Mitra P, Bokil H (2008) Observed brain dynamics. Oxford ; New York: Oxford University Press.

674 Murty DVPS, Shirhatti V, Ravishankar P, Ray S (2018) Large Visual Stimuli Induce Two Distinct
675 Gamma Oscillations in Primate Visual Cortex. J Neurosci 38:2730–2744.

676 Muthukumaraswamy SD, Edden RAE, Jones DK, Swettenham JB, Singh KD (2009) Resting GABA
677 concentration predicts peak gamma frequency and fMRI amplitude in response to visual
678 stimulation in humans. Proc Natl Acad Sci 106:8356–8361.

679 Muthukumaraswamy SD, Liley DTJ (2018) 1/f electrophysiological spectra in resting and drug-
680 induced states can be explained by the dynamics of multiple oscillatory relaxation processes.
681 NeuroImage 179:582–595.

682 Muthukumaraswamy SD, Singh KD, Swettenham JB, Jones DK (2010) Visual gamma oscillations and
683 evoked responses: Variability, repeatability and structural MRI correlates. NeuroImage
684 49:3349–3357.

685 Owsley C (2011) Aging and vision. Vision Res 51:1610–1622.

686 Palop JJ, Mucke L (2016) Network abnormalities and interneuron dysfunction in Alzheimer disease.
687 Nat Rev Neurosci 17:777–792.

688 Pantazis D, Fang M, Qin S, Mohsenzadeh Y, Li Q, Cichy RM (2018) Decoding the orientation of
689 contrast edges from MEG evoked and induced responses. NeuroImage 180:267–279.

690 Pesaran B, Pezaris JS, Sahani M, Mitra PP, Andersen RA (2002) Temporal structure in neuronal
691 activity during working memory in macaque parietal cortex. Nat Neurosci 5:805–811.

692 Podvalny E, Noy N, Harel M, Bickel S, Chechik G, Schroeder CE, Mehta AD, Tsodyks M, Malach R
693 (2015) A unifying principle underlying the extracellular field potential spectral responses in
694 the human cortex. J Neurophysiol 114:505–519.

695 Ray S, Maunsell JHR (2015) Do gamma oscillations play a role in cerebral cortex? Trends Cogn Sci
696 19:78–85.

697 Salat DH, Buckner RL, Snyder AZ, Greve DN, Desikan RSR, Busa E, Morris JC, Dale AM, Fischl B (2004)
698 Thinning of the Cerebral Cortex in Aging. Cereb Cortex 14:721–730.

699 Sheehan TC, Sreekumar V, Inati SK, Zaghloul KA (2018) Signal Complexity of Human Intracranial EEG
700 Tracks Successful Associative-Memory Formation across Individuals. J Neurosci 38:1744–
701 1755.

702 Shirhatti V, Borthakur A, Ray S (2016) Effect of Reference Scheme on Power and Phase of the Local
703 Field Potential. Neural Comput 28:882–913.

704 Sohal VS, Zhang F, Yizhar O, Deisseroth K (2009) Parvalbumin neurons and gamma rhythms enhance
705 cortical circuit performance. Nature 459:698–702.

706 Tada M, Nagai T, Kirihara K, Koike S, Suga M, Araki T, Kobayashi T, Kasai K (2014) Differential
707 Alterations of Auditory Gamma Oscillatory Responses Between Pre-onset High-risk
708 Individuals and First-episode Schizophrenia. Cereb Cortex:bhu278.

709 Uhlhaas PJ, Singer W (2007) What Do Disturbances in Neural Synchrony Tell Us About Autism? Biol
710 Psychiatry 62:190–191.

711 Vaden RJ, Hutcheson NL, McCollum LA, Kentros J, Visscher KM (2012) Older adults, unlike younger
712 adults, do not modulate alpha power to suppress irrelevant information. NeuroImage
713 63:1127–1133.

714 Veit J, Hakim R, Jadi MP, Sejnowski TJ, Adesnik H (2017) Cortical gamma band synchronization
715 through somatostatin interneurons. Nat Neurosci 20:951–959.

716 Verret L, Mann EO, Hang GB, Barth AMI, Cobos I, Ho K, Devidze N, Masliah E, Kreitzer AC, Mody I,
717 Mucke L, Palop JJ (2012) Inhibitory Interneuron Deficit Links Altered Network Activity and
718 Cognitive Dysfunction in Alzheimer Model. Cell 149:708–721.

719 Voytek B, Kramer MA, Case J, Lepage KQ, Tempesta ZR, Knight RT, Gazzaley A (2015) Age-Related
720 Changes in 1/f Neural Electrophysiological Noise. J Neurosci 35:13257–13265.

721 Wilson TW, Rojas DC, Reite ML, Teale PD, Rogers SJ (2007) Children and Adolescents with Autism
722 Exhibit Reduced MEG Steady-State Gamma Responses. Biol Psychiatry 62:192–197.

723 Yuval-Greenberg S, Tomer O, Keren AS, Nelken I, Deouell LY (2008) Transient Induced Gamma-Band
724 Response in EEG as a Manifestation of Miniature Saccades. Neuron 58:429–441.

725

726

Figure legends

Figure 1. Slow and fast gamma in an example elderly subject. a) Trial-averaged EEG trace (1st row, blue); time-frequency spectrograms of raw power (2nd row) and change in power from baseline (3rd row); and change in power with time (4th row) in alpha (8-12 Hz, blue), slow (20-34 Hz, pink) and fast gamma (36-66 Hz, orange) bands averaged across 10 unipolar (left column) and 9 bipolar (right column) electrodes. Vertical dashed lines represent actual stimulus duration (0-0.8 s, black) and period used for analysis within stimulus duration (0.25-0.75 s, red). Horizontal lines represent baseline (-0.5-0 s, black) and stimulus (0.25-0.75 s, red) analysis periods. Grey lines in spectrograms represent slow (solid) and fast (dashed) gamma frequency ranges. b) Right ordinate shows raw power spectral densities (PSDs, black traces) vs frequency in baseline (dotted) and stimulus (solid) periods averaged across 10 unipolar electrodes (left column) and 9 bipolar (right column) electrodes; left ordinate shows the same for change in PSD (in dB, solid blue trace) in stimulus period from baseline. Solid pink lines and dashed orange lines represent slow and fast gamma bands respectively. c) Scalp maps showing 112 bipolar electrodes (represented as disks). Colour of each disk represents change in slow (left) and fast (right) gamma power. 9 electrodes used in 1a and 1b above are marked with dots.

Figure 2. Baseline PSDs, slopes and alpha power. a) PSDs (averaged across 10 unipolar parieto-occipital and occipital electrodes) during baseline period averaged across analyzed (blue trace, n=343) and discarded (red trace, n=67) blocks (total 410 for all subjects recruited in the experiment: 149 elderly and 46 young). Thickness indicates SEM across blocks. Vertical solid and dashed lines indicate slow and fast gamma ranges respectively. b) Mean baseline PSDs for three age-groups on a log-log scale for unipolar (left) and bipolar (right) reference.

Thickness of traces indicate SEM across subjects. Age-group limits and the number of subjects in the respective age-groups are indicated on the left plot. c) Same as in 2b, but for males and females, pooled across all age-groups. d) Mean baseline PSDs for three ranges of baseline alpha power (<0.39, 0.39-0.79 and >0.79 units in 8-12 Hz) pooled across all age-groups. Thickness of traces and numbers indicate SEM across subjects and number of subjects in respective alpha power ranges.

Figure 3. Slow and fast gamma in younger and elderly subjects. a) Scatter plot showing change in slow (abscissa) and fast (ordinate) gamma power. Dotted lines represent 0.5 dB threshold. Points represent subjects with no gamma (dark blue), only slow gamma (light blue), only fast gamma (green) and both gamma rhythms (yellow) with change in power above 0.5 dB threshold. b) Change in PSDs vs frequency averaged across subjects (numbers denoted by N) as categorized in 3a. Thickness of traces indicate SEM. Solid pink and dashed lines represent slow and fast gamma ranges respectively. c) Bar plot showing percentage of subjects in three age-groups (marked by respective colours) categorized as in 3a. d) Schematic showing placements of left and right anterolateral and posteromedial group of electrodes used for analysis on the scalp, as well as ground and reference electrodes. e) Average scalp maps of 112 bipolar electrodes (disks) for three age-groups for slow (top row) and fast (bottom row) gamma. Colour of disks represents change in respective gamma power. Electrode groups represented as in 3d.

Figure 4. Change in gamma power vs age for anterolateral group of electrodes. Mean time-frequency change in power spectrograms (4a) and change in power spectra vs frequency (4b) for three age-groups separately for males (top row) and females (bottom row). Thickness of traces in 4b indicates SEM. Solid and dashed lines indicate slow and fast gamma frequency ranges respectively. c) Left column: bar plots showing mean change in slow gamma power for three age-groups separately for males and females. Number of subjects for respective age-groups are indicated on top. Error bars indicate SEM. Right column: scatter plot for change in slow gamma power vs age for all elderly subjects (>49 years age-group, N=128). Black line indicates regression fit. d) Same as in (4c) but for fast gamma.

Figure 5. Change in gamma power vs age for posteromedial group of electrodes. Same format as in Figure 4.

Figure 6. Centre frequency of slow and fast gamma vs age for elderly subjects. a) change in power vs frequency for 128 elderly subjects arranged in ascending order of age. Age for each subject is indicated on ordinate. Colour represents change in power in dB for each frequency. Circles and triangles represent centre frequency of slow and fast gamma rhythms respectively, indicated only for those subjects who have change in power in respective gamma range above 0.5 dB. b) Scatter plots showing centre frequency vs age for slow (top row) and fast (bottom row) gamma. Solid lines in both (6a) and (6b) are regression fits for centre frequency vs age. Left and right columns show analysis for anterolateral and posteromedial group of electrodes respectively.

Figure 7. Eye position, microsaccades and pupillary reactivity across age for elderly subjects. a) Eye-position in horizontal (top row) and vertical (middle row) directions; and histogram showing microsaccade rate (bottom row) vs time (-0.5-0.75 s of stimulus onset) for elderly subjects (n=127). Number of subjects in each age-group is indicated on top. Thickness indicates SEM. b) Main sequence showing peak velocity and maximum displacement of all microsaccades (number indicated by n) extracted for both elderly age-groups. Average microsaccade rate (mean±SEM) across all subjects for each elderly age-group is also indicated. c) Scatter plot showing change in power vs age for slow (top row) and fast (bottom row) gamma for all elderly subjects with analysable data after removal of trials containing microsaccades. Solid lines indicate regression fits. Numbers of subjects with analysable data in each age-group is indicated on top. d) Scatter plots for coefficient of variation (CV) of pupil diameter vs age (top row), change in slow (middle row) and fast (bottom row) gamma power. Pearson correlation coefficients (r) and p-values are also indicated.

Figure 8. Change in SSVEP power vs age for posteromedial group of electrodes. Time-frequency change in power spectrograms (8a) and change in power spectra vs frequency (8b) for three age-groups separately for males (top row) and females (bottom row). Thickness of traces in 8b indicates SEM. Insets in 8b display zoomed-in images of respective main plots, showing clear SSVEP peaks at 32 Hz. c) Top row: bar plots showing mean change in SSVEP power for three age-groups separately for males and females; Numbers of subjects in each age-group is indicated on top. Error bars indicate SEM. Bottom row: scatter plot for change in SSVEP power vs age for all elderly subjects (>49 years age-group, N=98). Black line indicates regression fit. d) Scalp maps for 112 electrodes (disks) averaged across all subjects separately for three age-groups. Colour indicates change in SSVEP power at 32 Hz for each electrode.

Supplementary Figure 1. PSD slopes (16-44 Hz) across age-groups, gender and baseline alpha power

a) Bar plots showing mean slopes of baseline PSDs for three age-groups separately for males and females in 16-44 Hz range for unipolar (left) and bipolar (right) reference. Error bars indicate SEM. Numbers on top indicate number of subjects. b) Scatter plot showing baseline slopes in 16-44 Hz range vs alpha power, for unipolar (left) and bipolar (right) reference for all 172 subjects used for analysis (128 elderly and 44 young). Lines indicate regression fits. Pearson correlation coefficients (r) and p-values are also indicated.

Figure 1

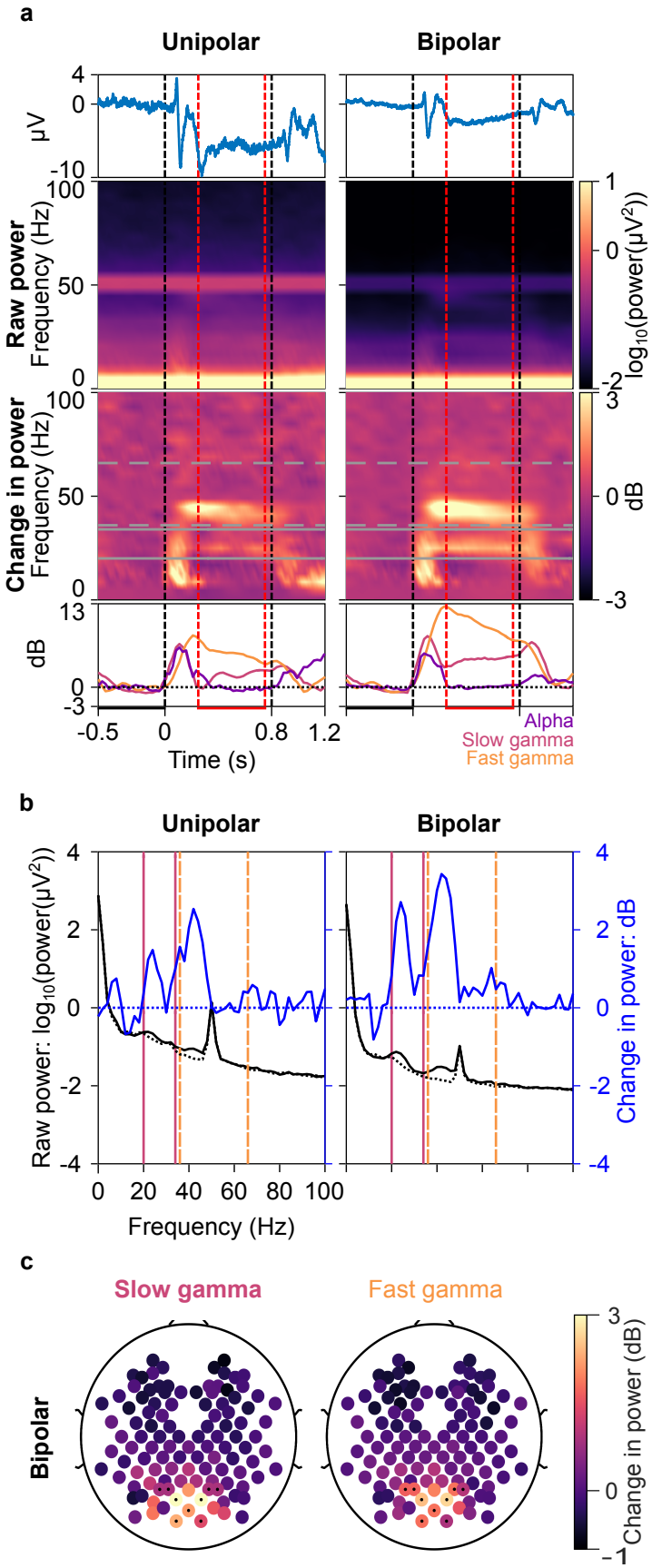
a
Unipolar
Bipolar
μV
4
0
-10
Raw power
Frequency (Hz)
100
50
0
1
0
-2
log10(power(μV²))
Change in power
Frequency (Hz)
100
50
0
3
0
-3
dB
dB
13
0
-3
-0.5
0
0.8
1.2
Time (s)
Alpha
Slow gamma
Fast gamma
b
Unipolar
Bipolar
Raw power: log10(power(μV²))
4
2
0
-2
-4
Change in power: dB
4
2
0
-2
-4
0
20
40
60
80
100
Frequency (Hz)
c
Slow gamma
Fast gamma
Bipolar
3
0
-1
Change in power (dB)

Figure 2

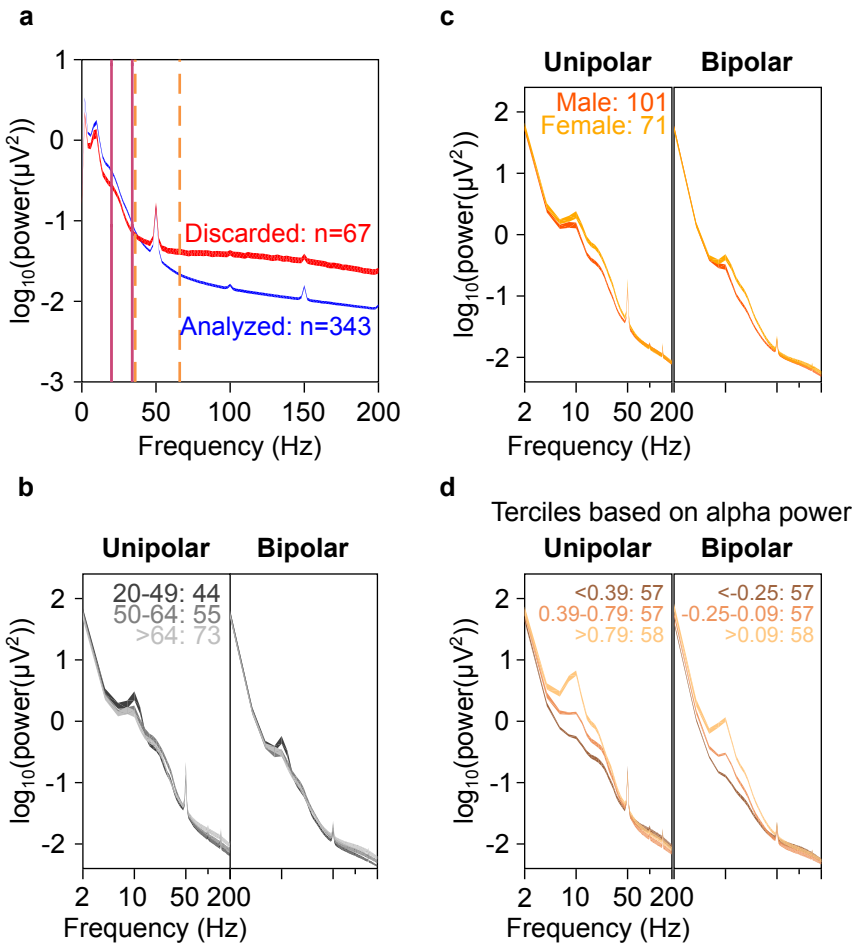
a
log10(power(μV²))
Discarded: n=67
Analyzed: n=343
Frequency (Hz)
c
Unipolar
Bipolar
Male: 101
Female: 71
Frequency (Hz)
b
Unipolar
Bipolar
20-49: 44
50-64: 55
>64: 73
Frequency (Hz)
d
Terciles based on alpha power
Unipolar
Bipolar
<0.39: 57
0.39-0.79: 57
>0.79: 58
<-0.25: 57
-0.25-0.09: 57
>0.09: 58
Frequency (Hz)

Figure 3

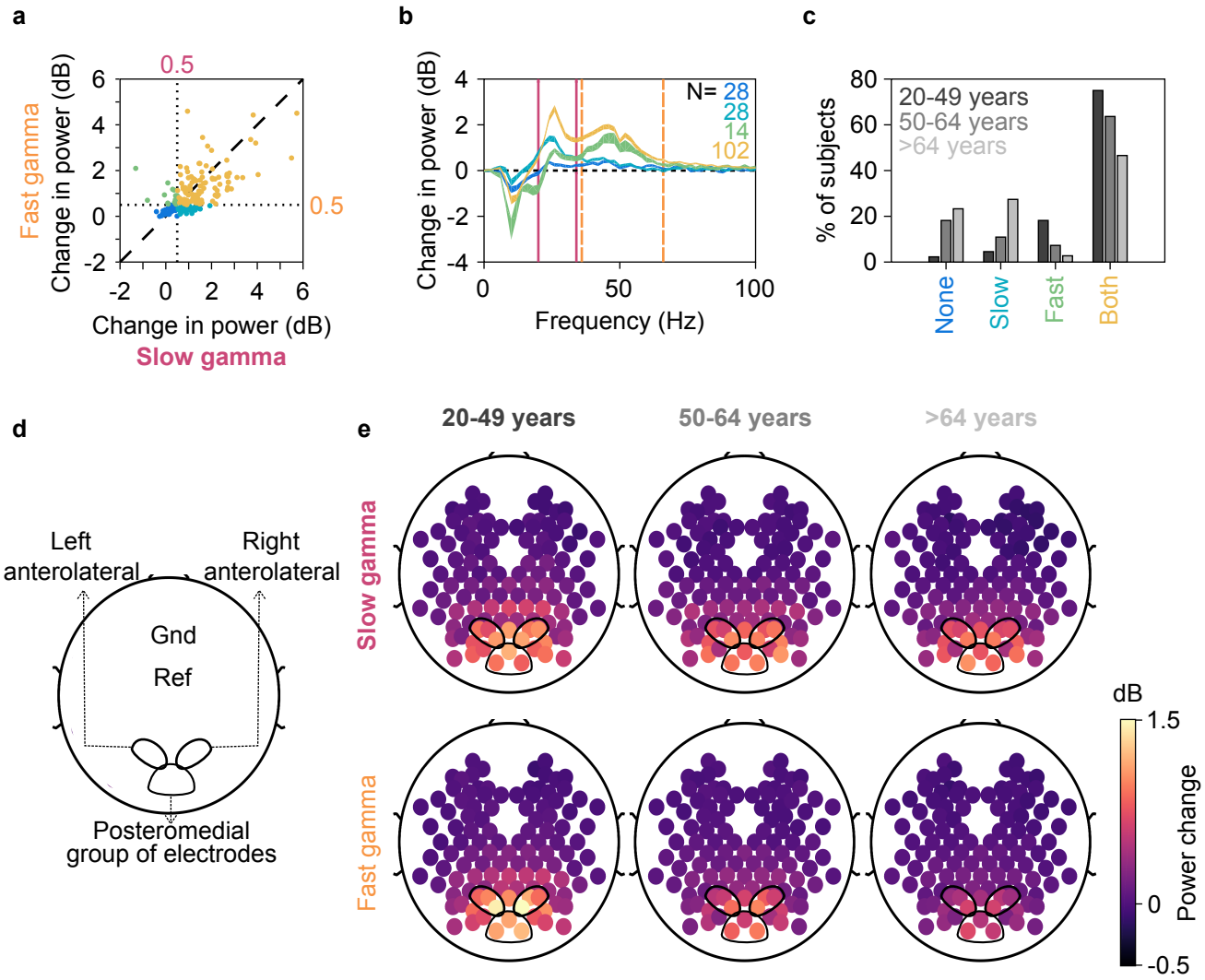
a
0.5
0.5
Fast gamma
Change in power (dB)
Change in power (dB)
Slow gamma
b
N= 28
28
14
102
Change in power (dB)
Frequency (Hz)
c
20-49 years
50-64 years
>64 years
% of subjects
None
Slow
Fast
Both
d
Left anterolateral
Right anterolateral
Gnd
Ref
Posteromedial group of electrodes
e
20-49 years
50-64 years
>64 years
Slow gamma
Fast gamma
dB
1.5
0
-0.5
Power change

Figure 4

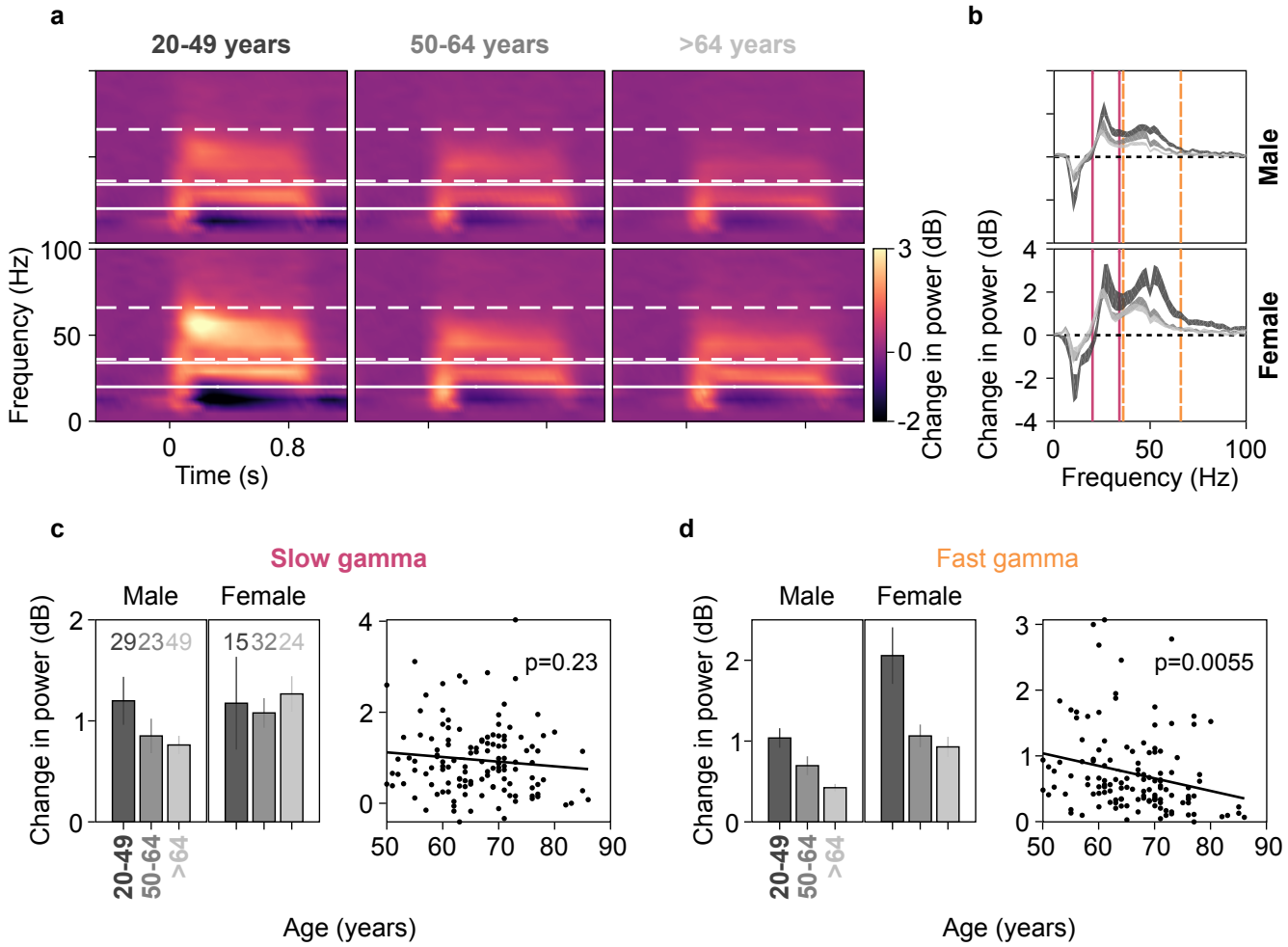
a
20-49 years
50-64 years
>64 years
Frequency (Hz)
100
50
0
0
0.8
Time (s)
3
0
-2
Change in power (dB)
b
Male
Female
Change in power (dB)
4
2
0
-2
-4
0
50
100
Frequency (Hz)
c
Slow gamma
Male
Female
Change in power (dB)
2
1
0
29 23 49
15 32 24
20-49
50-64
>64
4
2
0
p=0.23
50
60
70
80
90
Age (years)
d
Fast gamma
Male
Female
Change in power (dB)
2
1
0
20-49
50-64
>64
3
2
1
0
p=0.0055
50
60
70
80
90
Age (years)

Figure 5

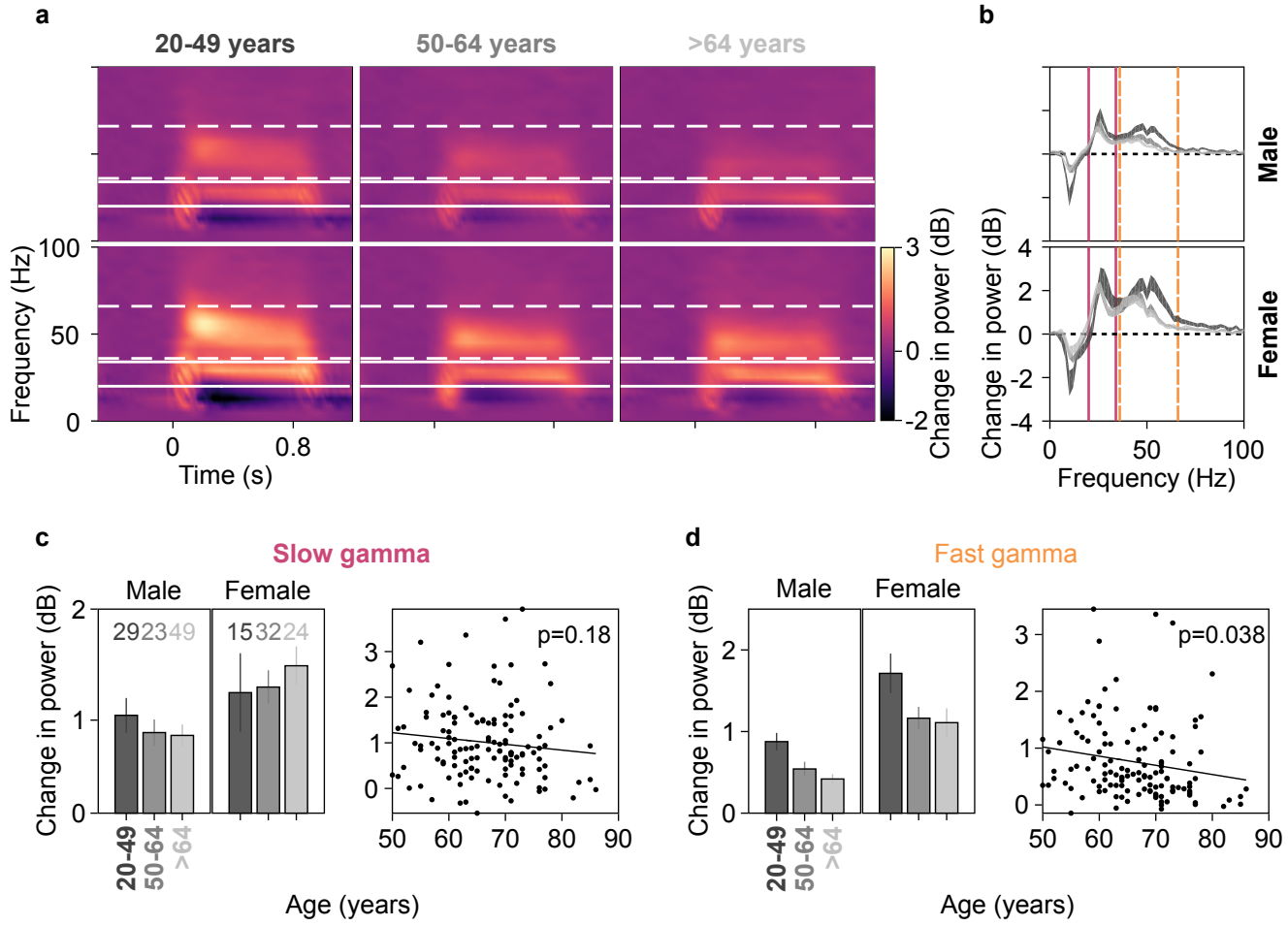
a
20-49 years
50-64 years
>64 years
Frequency (Hz)
100
50
0
0
0.8
Time (s)
3
0
-2
Change in power (dB)
b
Male
Female
Change in power (dB)
4
2
0
-2
-4
0
50
100
Frequency (Hz)
c
Slow gamma
Male
Female
Change in power (dB)
2
1
0
2923
49
1532
24
20-49
50-64
>64
p=0.18
3
2
1
0
50
60
70
80
90
Age (years)
d
Fast gamma
Male
Female
Change in power (dB)
2
1
0
20-49
50-64
>64
p=0.038
3
2
1
0
50
60
70
80
90
Age (years)

Figure 6

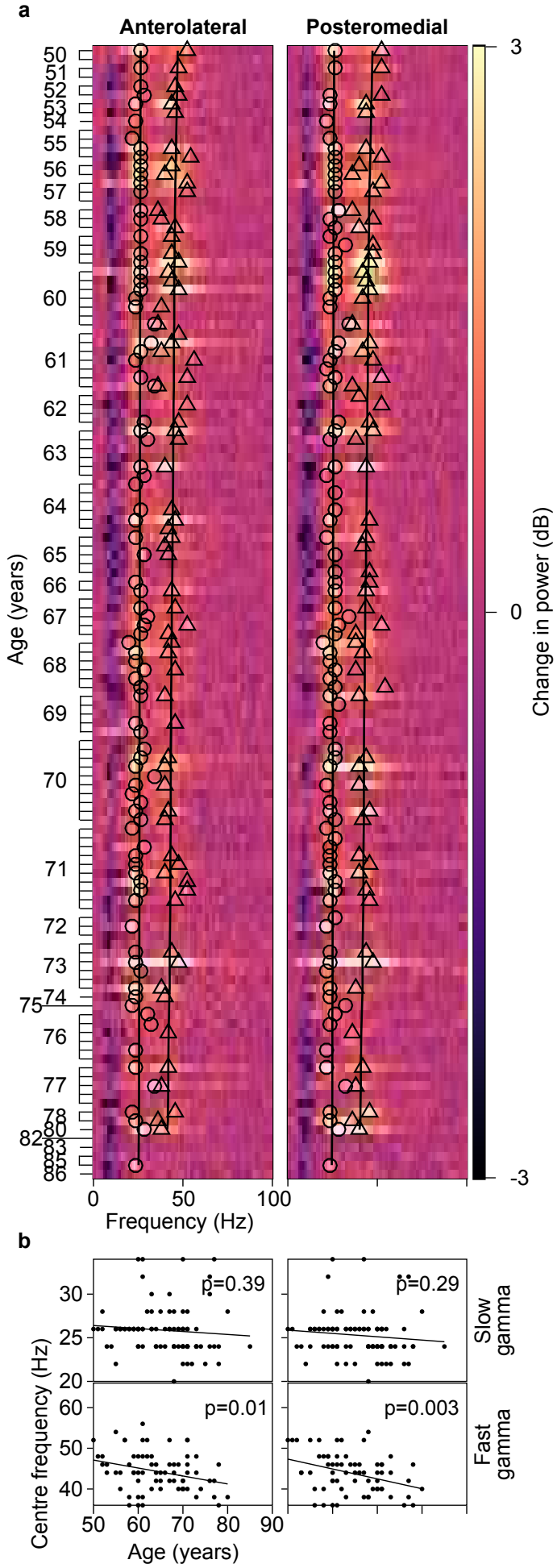
a
Anterolateral
Posteromedial
Age (years)
Frequency (Hz)
Change in power (dB)
3
0
-3
b
p=0.39
p=0.29
p=0.01
p=0.003
Slow gamma
Fast gamma
Centre frequency (Hz)
Age (years)

Figure 7

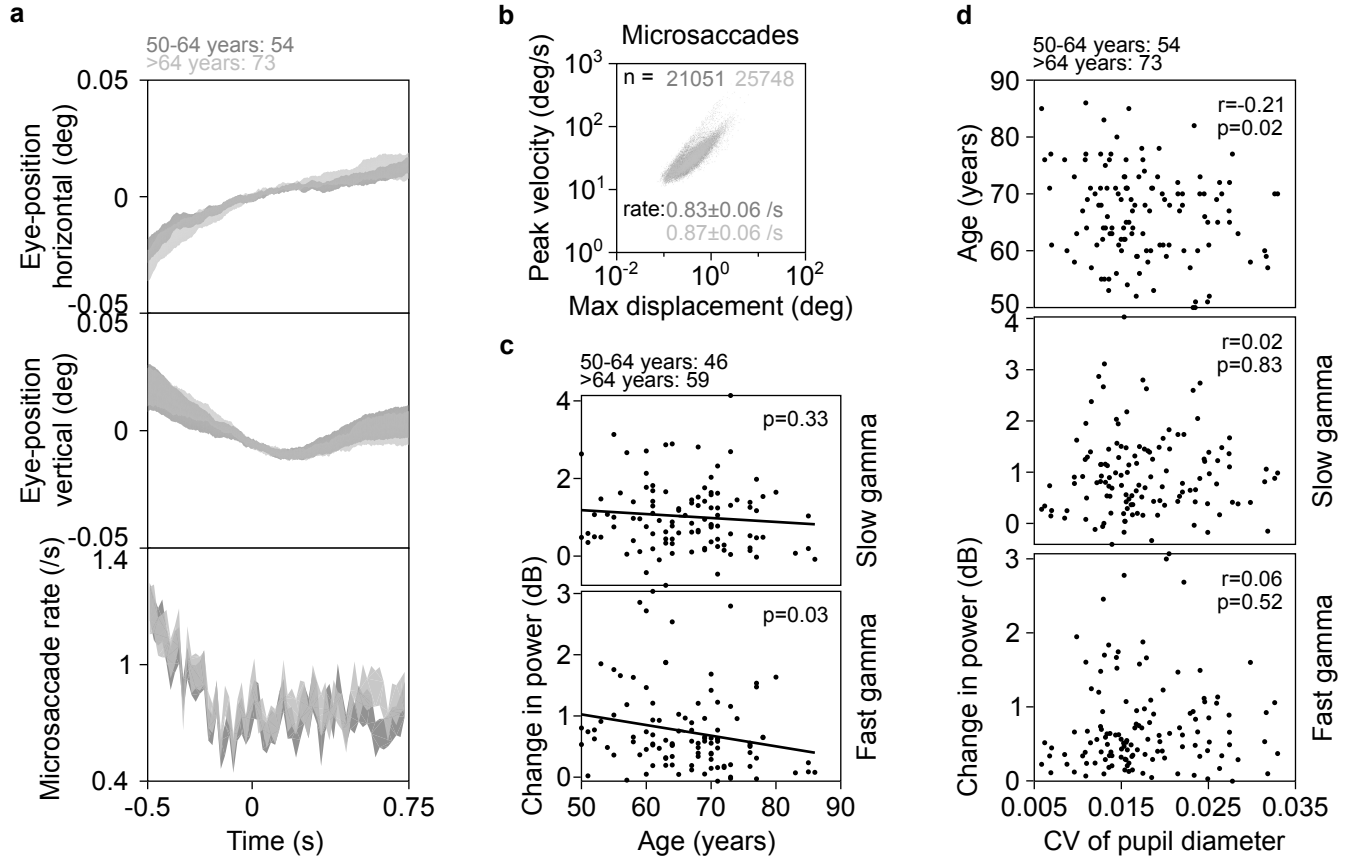
a
50-64 years: 54
>64 years: 73
Eye-position horizontal (deg)
Eye-position vertical (deg)
Microsaccade rate (/s)
Time (s)
b
Microsaccades
n = 21051 25748
rate:0.83±0.06 /s
0.87±0.06 /s
Peak velocity (deg/s)
Max displacement (deg)
c
50-64 years: 46
>64 years: 59
p=0.33
p=0.03
Slow gamma
Fast gamma
Change in power (dB)
Age (years)
d
50-64 years: 54
>64 years: 73
r=-0.21
p=0.02
r=0.02
p=0.83
r=0.06
p=0.52
Age (years)
Slow gamma
Fast gamma
Change in power (dB)
CV of pupil diameter

Figure 8

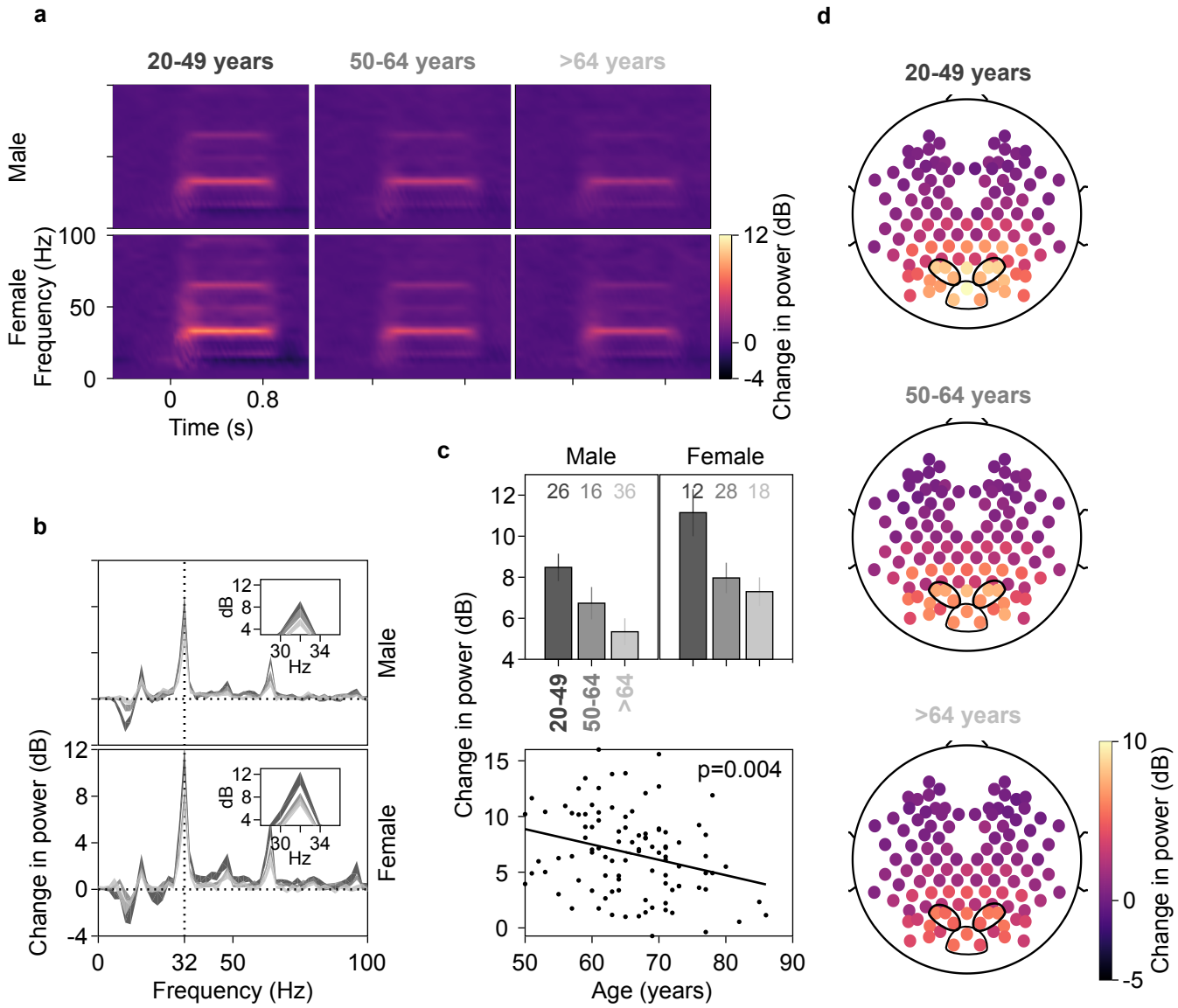
a
20-49 years
50-64 years
>64 years
Male
Female
Frequency (Hz)
100
50
0
0
0.8
Time (s)
12
0
-4
Change in power (dB)
b
Male
Female
Change in power (dB)
12
8
4
0
-4
0
32
50
100
Frequency (Hz)
dB
30
34
Hz
c
Male
Female
26 16 36
12 28 18
20-49
50-64
>64
Change in power (dB)
p=0.004
Age (years)
d
20-49 years
50-64 years
>64 years
10
0
-5
Change in power (dB)
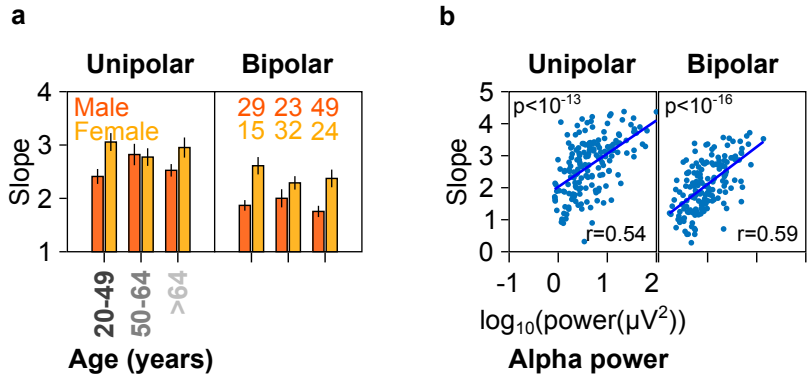
Supplementary Figure 1